Solar Energy Materials & Solar Cells 130 (2014) 241–245

Contents lists available at ScienceDirect

Solar Energy Materials & Solar Cells

journal homepage: www.elsevier.com/locate/solmat

Analysis of InAs/GaAs quantum dot solar cells using Suns-V_{oc} measurements

N.S. Beattie [a,*], G. Zoppi [a], P. See [b], I. Farrer [c], M. Duchamp [d], D.J. Morrison [e], R.W. Miles [a], D.A. Ritchie [c]

[a] Northumbria Photovoltaics Applications Group, Northumbria University, Newcastle upon Tyne, NE1 8ST, United Kingdom
[b] National Physical Laboratory, Teddington, TW11 0LW, United Kingdom
[c] Cavendish Laboratory, University of Cambridge, Cambridge CB3 0HE, United Kingdom
[d] Ernst Ruska-Centre for Microscopy and Spectroscopy with Electrons and Peter Grünberg Institute, Forschungszentrum Jülich, D-52425 Jülich, Germany
[e] Solar Capture Technologies, Albert Street, Blyth, NE24 1LZ, United Kingdom

ARTICLE INFO

Article history:
Received 30 May 2014
Received in revised form
11 July 2014
Accepted 14 July 2014
Available online 6 August 2014

Keywords:
InAs quantum dots
Concentrator
Solar cell

ABSTRACT

The performance of InAs/GaAs quantum dot solar cells was investigated up to an optical concentration of 500-suns. A high temperature spacer layer between successive layers of quantum dots was used to reduce the degradation in the open circuit voltage relative to a control device without quantum dots. This improvement is explained using optical data while structural imaging of quantum dot stacks confirm that the devices are not limited by strain. The evolution of the open circuit voltage as a function of number of suns concentration was observed to be nearly ideal when compared with a high performance single junction GaAs solar cell. Analysis of Suns-V_{oc} measurements reveal diode ideality factors as low as 1.16 which is indicative of a low concentration of defects in the devices.

1. Introduction

The inclusion of stacked layers of InAs self-assembled quantum dots within the intrinsic region of a GaAs *p-i-n* diode has led to the development of a new type of quantum dot solar cell (QDSC) [1–4]. The flexibility afforded by this system makes it an attractive prototype for realising the intermediate band solar cell [5]. Adding the quantum dots to the structure creates a narrow band of states within the energy band gap of the host GaAs and the capture of sub-band gap photons provides an additional contribution to the photocurrent. The challenge of using this system to realise the intermediate band solar cell is maintaining quasi-Fermi level separation between the quantum dots and the conduction band [6,7].

Irrespective of the goal to realise an intermediate band solar cell, QDSCs have shown recent promise reaching solar energy conversion efficiency of 18.7% under air mass (AM) 1.5 conditions with an anti-reflective coating [8]. It has also been suggested that exceeding the fundamental Shockley–Queisser limit [9] is possible with this type of solar cell relying on single photon absorption only [10] although this is a source of debate [11].

Generally, reports of QDSCs show an extended external quantum efficiency (EQE) at long wavelengths and reduced open circuit voltage V_{oc}, relative to a GaAs control device without quantum dots. The degradation in V_{oc} arises from a reduction in the total energy band gap primarily due to the InAs wetting layer near the conduction band and an effective continuum of closely packed confined levels near the valence band that can be considered as an offset [12]. The discrete energy levels within the quantum dots themselves also provide an additional path for recombination which serves to reduce V_{oc}. Taken together, these effects reduce the effective band gap to approximately 1.3 eV [13]. A further source of recombination is through strain-related defects which exacerbates the reduction in V_{oc}. Efforts to reduce this strain include the addition of strain balancing layers [14–17] and the best QDSCs now have comparable performance to control devices at 1-sun irradiance.

There are, however, only a limited number of reports of QDSCs under concentrated sunlight. One such study analysed the evolution of V_{oc} up to 10-suns and found a variation in the obtained diode ideality factor n, that depended on the thickness of spacer layer between consecutive layers of quantum dots [8]. In another study up to 450-suns the ideality factor was found to be $n=1.4$ which is indicative of Shockley–Read–Hall recombination in the depletion region [18]. It has also been shown that within the intermediate band theory, voltage recovery occurs with increasing concentration for a QDSC relative to a control device but only at low temperatures [19].

Following the initial optimisation of InAs/GaAs QDSCs at 1-sun, Suns-V_{oc} measurements are used to assess the potential for QDSCs as concentrator solar cells and to gain fundamental insight into the

* Corresponding author.
E-mail address: neil.beattie@northumbria.ac.uk (N.S. Beattie).

http://dx.doi.org/10.1016/j.solmat.2014.07.022

device performance. The evolution of V_{oc} with concentration points to low diode ideality factors indicating a low concentration of defects and confirms that this is an essential requirement for the development of QDSCs.

2. Materials and methods

GaAs *p-i-n* QDSC wafers were grown using molecular beam epitaxy (MBE). The structures included 250 nm of *n*-GaAs deposited on an $n+$ substrate followed by 1000 nm of *n*-GaAs. A further 150 nm GaAs spacer layer was then grown before the deposition of two monolayers of InAs resulted in the formation of self-assembled InAs quantum dots via the Stranski–Krastanov growth mode. These were capped with a 35 nm GaAs spacer layer before growing a further layer of InAs quantum dots. By repeating this sequence, a stack of 20 layers of quantum dots was created in the intrinsic region of the diode comprising a total thickness of 700 nm. The structure was completed by the addition of 200 nm of *p*-GaAs, a 50 nm AlGaAs window layer and a $p+$ cap. For the purposes of comparison a control wafer was also grown without the quantum dot stack in the intrinsic region. All other growth parameters remained the same for the control. Photolithography was used to fabricate QDSC and control devices of circular geometry ranging from 2 to 4 mm diameter. No area-related performance variation was observed in the results. Au/Ge/Ni metalisation to the $n+$ substrate formed the back ohmic contact while a Al/Ti/Au metallic grid formed a front contact. The grid area for a 3.0 mm diameter device was 1.1 mm^2 or 15.6% of the cell area. An anti-reflective coating was not applied to any of the devices.

In order to characterise the optical properties of the quantum dots, calibration wafers were also grown by MBE. These were not diode structures but simply stacked layers of quantum dots with 35 nm spacer layers designed to mimic the intrinsic region of the QDSC devices. The calibration wafers were studied using room temperature photoluminescence (PL). The PL setup used a chopped 532 nm laser and a Horiba iHR320 monochromator with a dual colour solid state detector operating in a lock-in configuration.

1-sun current-density versus voltage (*JV*) measurements were performed under AM1.5 conditions (100 mW cm^{-2}) using an Abet Technologies solar simulator and a Keithley sourcemeter. External quantum efficiency (EQE) measurements were made using a tungsten white light source and a Bentham Instruments monochromator. Chopped monochromatic light was focused onto to solar cells and the resulting photocurrent was measured using a lock-in amplifier with current pre-amplification.

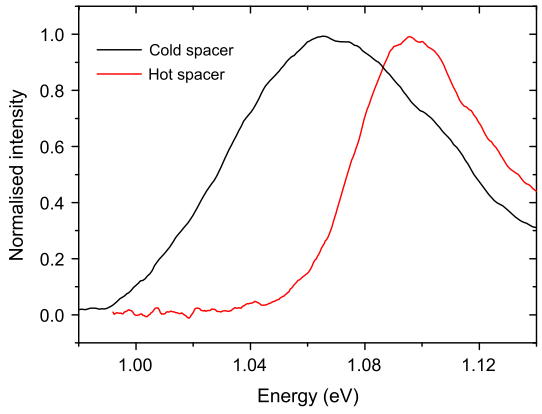

Fig. 1. Normalised photoluminescence spectra from two different quantum dot stacks. The entire spacer layer for the stack referred to as "cold spacer"was grown at 470 °C whereas for the sample labelled "hot spacer" the first 5 nm was grown at 470 °C and the remaining 30 nm at 580 °C.

Concentration measurements were made using a Suns-V_{oc} system from Sinton Instruments. This apparatus uses a xenon flashlamp to simultaneously measure V_{oc} and light intensity within a few milliseconds. These data can be used to construct a pseudo-*JV* curve by noting that at each open circuit voltage, the implied light-generated current is given by $J = J_{sc}(1-X)$, where J_{sc} is the short circuit current and X is the number of suns concentration [20]. In this analysis J_{sc} is assumed to vary linearly with light intensity. The difference between the pseudo and actual *JV* curves is series resistance and this technique therefore yields an upper limit of solar cell efficiency.

3. Results and discussion

3.1. Device optimisation

Stacking layers of InAs quantum dots within the intrinsic region of the GaAs diode can cause a build up of strain within the stack that is detrimental to solar cell performance [6,21]. To address this issue, a relatively thick GaAs spacer layer was used such that vertical propagation of strain-related defects is reduced. In addition, the spacer layer was partially grown at higher temperature to counteract any non-uniformity in quantum dot size that may result from strain [22]. Fig. 1 shows the normalised PL spectra from two calibration wafers which were designed to assess the quality of the quantum dots. For the sample referred to as "cold spacer" the entire GaAs spacer layer was grown at 470 °C while for the "hot spacer" sample only the first 5 nm was grown at this temperature with the remaining 30 nm grown at 580 °C. It can be seen in Fig. 1 that the hot spacer layer results in a higher quantum dot ground state energy of 1.10 eV compared with 1.07 eV for the stack with the cold spacer. The higher ground state energy is characteristic of smaller quantum dots. Additionally, the full width at half maximum for the hot spacer stack is 55 meV compared with 86 meV for the cold spacer stack. Narrowed linewidth is evidence of more homogeneous quantum dots within the stack and provides some verification that vertical strain propagation in the structure (which would result in larger quantum dots higher up the stack) is absent.

Transmission electron microscope (TEM) images of quantum dot stacks grown with cold and hot spacer layers are shown in Fig. 2(a) and (b) respectively. In both of these figures the quantum dots appear as dark areas on a bright background and it is apparent that there is no strain-related vertical alignment or size non-uniformity. Importantly, the TEM images also show that the material is of a high quality with no dislocations or defects.

Having established appropriate growth conditions for the creation of a high quality quantum dot stack, device wafers were grown and processed into QDSCs. Fig. 3 shows the *JV* characteristics obtained under AM1.5 conditions for two QDSCs. These initial devices did not include the AlGaAs window layer and consequently have relatively low values of J_{sc}. From Fig. 3 it can be seen that partially growing the spacer at higher temperature has increased V_{oc} by 28% from 0.53 V to 0.68 V. This increase can be explained by the PL data which indicates that the hot spacer layer QDSC has smaller quantum dots with larger spacing between the levels resulting in a larger effective band gap for the device.

The basic photovoltaic (PV) device parameters extracted from the data shown in Fig. 3 are given in Table 1. Several devices of each type shown in Fig. 3 were tested and the parameters in Table 1 are representative of the set. While variations in J_{sc} could be attributed to processing variations the increase in fill factor (*FF*) was broadly observed across all of the hot spacer layer QDSCs. One possible reason for this is a reduction in shunt pathways created by having material with fewer strain-related defects.

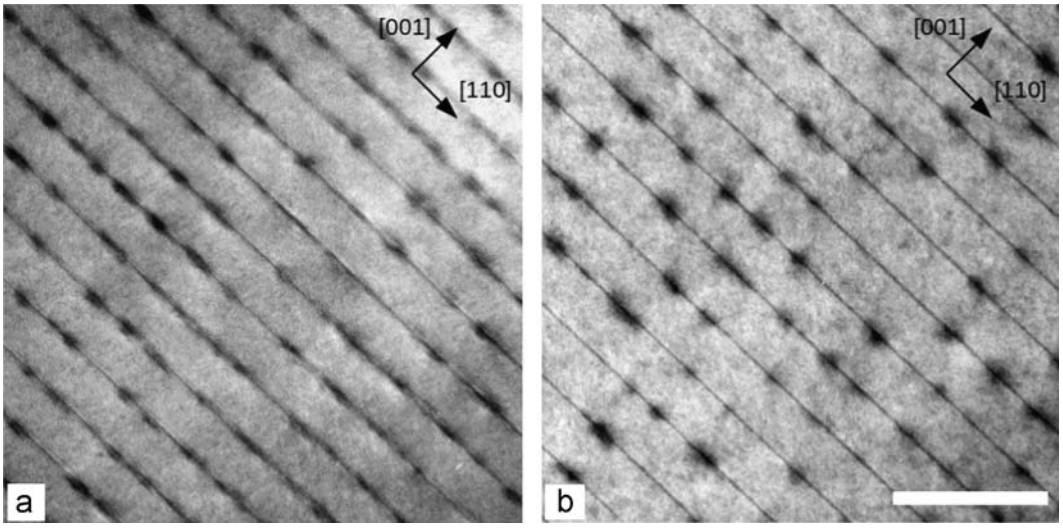

Fig. 2. TEM images taken under bright field conditions (2°) of a quantum dot stack with (a) cold spacer and (b) hot spacer between successive layers. The white scale bar is 100 nm.

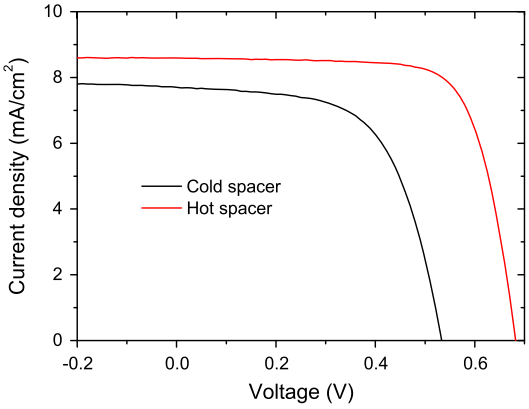

Fig. 3. Current density versus voltage characteristics for QDSC devices fabricated using hot and cold GaAs spacer layers in the InAs quantum dot stack.

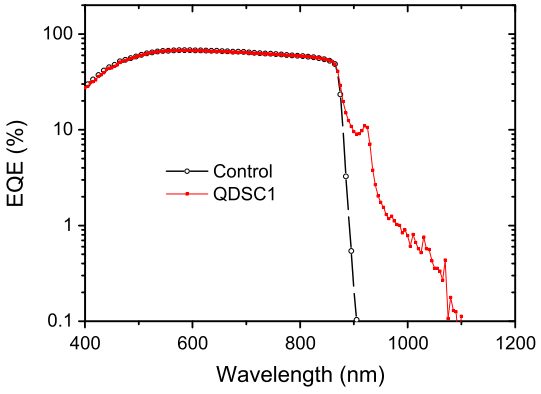

Fig. 4. External quantum efficiency spectra for an optimised QDSC (red line and filled squares) and a GaAs control device (black dashed line and open circles) without quantum dots. (For interpretation of the references to color in this figure caption, the reader is referred to the web version of this article.)

Table 1
PV device parameters for the QDSCs in Fig. 3.

Cell	V_{oc} (V)	J_{sc} (mA/cm^2)	FF	η (%)
Cold spacer	0.53	7.8	0.62	2.5
Hot spacer	0.68	8.6	0.72	4.3

Although an improvement in V_{oc} has been experimentally confirmed, the PV device efficiencies given in Table 1 are uncharacteristically low for III–V solar cells and indicate that significant device optimisation is required. To minimise surface recombination an AlGaAs window layer was inserted immediately below the $p+$ cap during the MBE growth. Additionally, the $p+$ cap was removed (apart from the region below the contacts) via chemical etching to improve light coupling into the device. These optimisation steps were performed for both QDSC and control devices alike and the EQE for the optimised devices is shown in Fig. 4. It can be seen from this figure that the inclusion of a quantum dot stack extends the EQE to longer wavelengths relative to a control device which does not contain quantum dots. The EQE response of the control device falls off rapidly around the GaAs band edge whereas sub-band gap photons are captured by the quantum dots giving rise to an EQE signal up to 1100 nm. The EQE signal for the QDSC shows a feature around 920 nm which is attributed to the InAs wetting layer. At room temperature, the additional photocurrent in the QDSC is the result of thermal activation of carriers from the quantum dots to the conduction band however this has recently been confirmed to be a two-photon process (as required by the intermediate band solar cell theory) at low temperature [23].

The *JV* characteristic for the optimised devices is shown in Fig. 5. Crucially, J_{sc} is ~4% greater than J_{sc} for a control device demonstrating the advantage of adding quantum dots to the structure. While V_{oc} has further increased relative to the first set of devices to 0.80 V, it is lower than the control solar cell. This is due to the overall band gap reduction created by the quantum dots and any other recombination pathways that remain in the structure. In this context it is notable that $V_{oc} = 1$ V has recently been achieved by using GaP and GaAsP strain balancing layers [14]. However, the results presented here suggest that the devices are not limited by strain. This is an important new insight because it suggests that strain balancing layers are perhaps not required to achieve high values of V_{oc} in QDSCs thereby reducing the complexity of the growth. Moreover, further investigation is required to understand more precisely the effect of strain-balancing layers on the nanostructure of the quantum dots.

The data in Fig. 5 have been fitted with the well-known double diode model:

$$J = J_L - J_{01}\left[\exp\left(\frac{qV}{k_BT}\right) - 1\right] + J_{02}\left[\exp\left(\frac{qV}{2k_BT}\right) - 1\right], \quad (1)$$

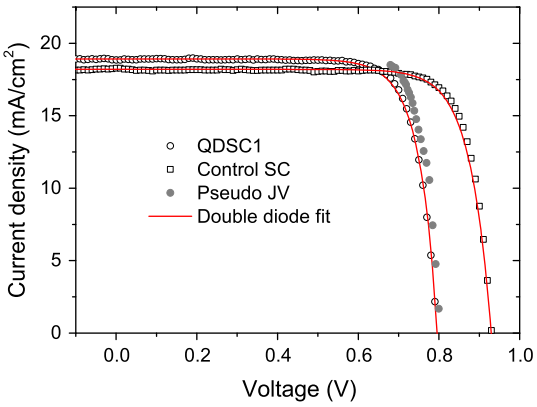

Fig. 5. Current density versus voltage characteristics for an optimised QDSC (open circles) and an optimised control device (open squares). Solid grey points show the pseudo-*JV* characteristic calculated from concentration measurements and red lines are fits to Eq. (1). (For interpretation of the references to color in this figure caption, the reader is referred to the web version of this article.)

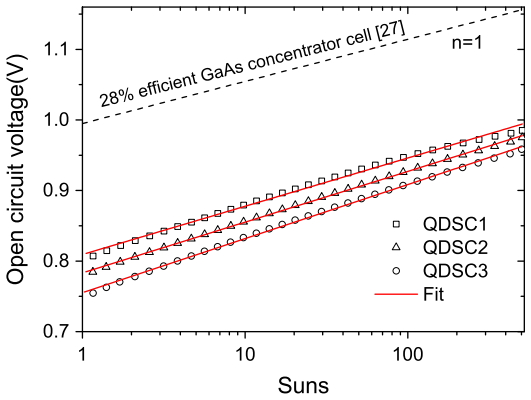

Fig. 6. V_{oc} versus number of suns concentration for three QDSCs and a single junction GaAs solar cell from reference [27]. Red lines are fits to Eq. (2). (For interpretation of the references to color in this figure caption, the reader is referred to the web version of this article.)

Table 2
PV device parameters for QDSC1 and control.

Cell	V_{oc} (V)	J_{sc} (mA/cm^2)	J_{01} (mA/cm^2)	J_{02} (mA/cm^2)	FF	η (%)
QDSC1	0.80	18.9	1.74×10^{-13}	3.18×10^{-6}	0.79	11.9
Control	0.93	18.2	7.33×10^{-16}	2.40×10^{-7}	0.80	13.5

Table 3
Diode ideality factors obtained from concentration data.

Cell	1-sun V_{oc} (V)	n	
		Suns$-V_{oc}$	J_{sc}vs.V_{oc}
QDSC1	0.80	1.15	1.16
QDSC2	0.78	1.21	1.21
QDSC3	0.75	1.29	1.25

where J_L is the light-generated photocurrent density and J_{01} and J_{02} are fitting parameters accounting for the diffusion current and recombination through defects respectively. These parameters and the PV device parameters are extracted from the data and shown in Table 2. The parameters are similar to other reported InAs/GaAs quantum dot solar cells [24,25] and provide a basis for experiments under concentrated sunlight.

3.2. Performance under concentrated irradiance

QDSCs were tested under concentrated illumination using the Suns-V_{oc} technique described earlier. In order to confirm the validity of this technique a pseudo-*JV* curve was constructed and compared with the actual *JV* curve obtained under AM1.5 conditions. The result of this step is shown in Fig. 5 where it can be seen that the pseudo-*JV* closely follows the characteristic for QDSC1 with the difference being series resistance which was determined to be $R_s = 1.57 \pm 0.09\ \Omega\ \mathrm{cm}^2$ and $R_s = 1.42 \pm 0.03\ \Omega\ \mathrm{cm}^2$ for QDSC1 and the control devices respectively. The pseudo-*JV* curve is constructed from data obtained during decaying irradiance which has a minimum value of $\sim 3\ \mathrm{mW/cm}^2$ and consequently the data do not reach the short circuit condition. However, this was obtained by comparing the 1-sun value with measurements from a calibrated reference cell that is integrated with the Suns-V_{oc} system.

The efficiency of a solar cell increases with concentration through the open circuit voltage and a simplified model is given as

$$V_{ocX} = V_{oc} + n\frac{k_B T}{q}\ln X, \tag{2}$$

where V_{ocX} is the open circuit voltage at X suns concentration, n is the diode ideality factor, q is the electronic charge and k_B is the Boltzmann's constant. Typically, for high performance GaAs concentrator solar cells, the rise in V_{oc} is initially controlled by recombination through defects ($n=2$) before crossing over to band-to-band recombination ($n=1$) in the high injection regime where V_{oc} is dominated by diffusion [26].

Fig. 6 shows the evolution of V_{oc} with concentration up to 500-suns for three quantum dot solar cells: QDSC1, QDSC2 and QDSC3. The data can all be described by Eq. (2) yielding diode factors that are close to unity as shown in Table 3. The agreement with the fit is less good at the highest concentration where series resistance becomes limiting. This can be addressed by optimising the top contact for concentrator applications. Diode factors close to unity are evidence of high quality material with a relatively low concentration of defects and are typical for high-performance GaAs concentrator solar cells. Diode factors of $n \simeq 1.4$ have been previously established for QDSCs from the evolution of V_{oc} with suns [18] however the values reported here are the lowest to date and are evidence of strong potential for QDSCs. Fig. 6 also shows the evolution of V_{oc} with concentration for a high efficiency, single junction GaAs concentrator solar cell [27]. With further optimisation of the quantum dot growth, V_{oc} can approach this reference allowing the additional photocurrent generated by the quantum dots to be more fully exploited.

J_{sc} values were also obtained from the Suns-V_{oc} measurements and plotted as a function of V_{oc} in Fig. 7. At high carrier concentrations, the double diode model is not applicable due to the distributed nature of series resistance [28] and therefore a single diode model has been fitted to this data. This step provides verification of the diode factors deduced from Fig. 6 and these are listed in Table 3. The agreement between the two methods confirms the earlier assumption that J_{sc} varies linearly across the range of concentration. A further observation is a general trend of $n \to 1$ as the 1-sun V_{oc} increases. This correlations supports the idea that the degradation of V_{oc} is caused by an increasing concentration of defects in the depletion region although it is possible that other mechanisms such as perimeter recombination can also cause a departure from ideality [29].

Finally, using the pseudo-*JV* curve obtained at 500-suns the best QDSC pseudo-efficiency was determined to be $\eta = 16.5\%$. This increases to $\eta = 19.5\%$ when shadowing losses from the top contact are taken into account. While this value does not include series resistance and therefore represents an upper limit, it demonstrates

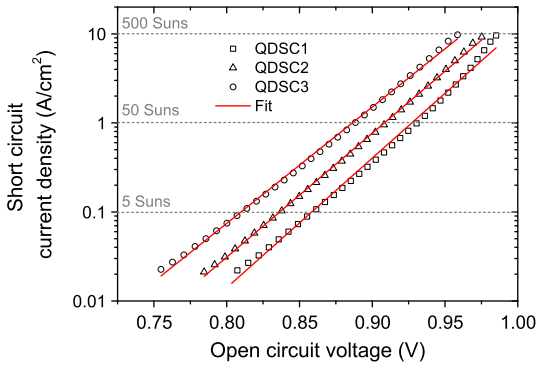

Fig. 7. J_{sc} versus V_{oc} for QDSC1-3. Red lines are fits to a single diode model. (For interpretation of the references to color in this figure caption, the reader is referred to the web version of this article.)

the potential opportunity for this novel technology. With further optimisation, including the application of an anti-reflective coating, it will be straightforward to increase the device efficiency above 20% under concentration.

4. Conclusions

In conclusion, by careful control of the wafer growth parameters it has been possible to increase V_{oc} for a QDSC relative to a control device without quantum dots. Structural data indicate that the devices are not limited by strain while analysis of optical data accounts for the increase in V_{oc}. Suns-V_{oc} measurements performed with QDSCs devices reveal low diode ideality factors typical of a high quality solar cell. Moreover, the evolution of V_{oc} with concentration is similar to a high efficiency single junction GaAs cell indicating that this technology has the potential to exceed the detailed balance limit if the issues around V_{oc} degradation can be resolved.

Acknowledgments

The authors acknowledge financial support from the European Union under the Seventh Framework Programme under a contract for an Integrated Infrastructure Initiative. Reference 312483 – ESTEEM2.

References

[1] A. Luque, A. Martí, N. López, E. Antolí, E. Cánovas, C. Stanley, C. Farmer, L.J. Caballero, L. Cuadra, J.L. Balenzategui, Experimental analysis of the quasi-Fermi level split in quantum dot intermediate-band solar cells, Appl. Phys. Lett. 87 (2005) 83505.
[2] R.B. Laghumavarapu, M. El-Emawy, N. Nuntawong, A. Moscho, L.F. Lester, D. L. Huffaker, Improved device performance of InAs/GaAs quantum dot solar cells with GaP strain compensation layers, Appl. Phys. Lett. 91 (2007) 243115.
[3] D. Zhou, P.E. Vullum, G. Sharma, S.F. Thomassen, R. Holmestad, T.W. Reenaas, B.O. Fimland, Positioning effects on quantum dot solar cells grown by molecular beam epitaxy, Appl. Phys. Lett. 96 (2010) 83108.
[4] J. Wu, F.M. Makableh, R. Vasan, M.O. Manasreh, B. Liang, C.J. Reyner, D. L. Huffaker, Strong interband transitions in InAs quantum dots solar cell, Appl. Phys. Lett. 100 (2012) 51907.
[5] A. Luque, A. Martí, Increasing the efficiency of ideal solar cells by photon induced transitions at intermediate levels, Phys. Rev. Lett. 78 (1997) 5014–5017.
[6] E. Antolín, A. Martí, C.D. Farmer, P.G. Linares, E. Hernández, A.M. Sánchez, T. Ben, S.I. Molina, C.R. Stanley, A. Luque, Reducing carrier escape in the InAs/GaAs quantum dot intermediate band gap solar cell, J. Appl. Phys. 108 (2010) 64513.
[7] A. Luque, A. Martí, The intermediate band solar cell: progress towards the realization of an attractive concept, Adv. Mater. 22 (2010) 160–174.
[8] K. Tanabe, D. Guimard, D. Bordel, Y. Arakawa, High-efficiency InAs/GaAs quantum dot solar cells by metal organic chemical vapor deposition, Appl. Phys. Lett. 100 (2012) 193905.
[9] W. Shockley, H.J. Queisser, Detailed balance limit of efficiency of p–n junction solar cells, J. Appl. Phys. 32 (1961) 510.
[10] G. Wei, K. Shiu, N.C. Giebink, S.R. Forrest, Thermodynamic limits of quantum photovoltaic cell efficiency, Appl. Phys. Lett. 91 (2007) 223507.
[11] A. Martí, A. Luque, Comment on Thermodynamics limits of quantum photovoltaic cell efficiency, Appl. Phys. Lett. 92 (2008) 66101.
[12] V. Popescu, G. Bester, M.C. Hanna, A.G. Norman, A. Zunger, Theoretical and experimental examination of the intermediate-band concept for strain-balanced (In,Ga)As/Ga(As,P) quantum dot solar cells, Phys. Rev. B 78 (2008) 205321.
[13] A. Martí, E. Antolí, E. Cánovas, N. López, P.G. Linares, A. Luque, C. Stanley, C. Farmer, Elements of the design and analysis of quantum-dot intermediate band solar cells, Thin Solid Films 516 (2008) 6716.
[14] C.G. Bailey, D.V. Forbes, R.P. Raffaelle, S.M. Hubbard, Near 1V open circuit voltage InAs/GaAs quantum dot solar cells, Appl. Phys. Lett. 98 (2011) 163105.
[15] S.M. Hubbard, C.D. Cress, C.G. Bailey, R.P. Raffaelle, S.G. Bailey, D.M. Wilt, Effect of strain compensation on quantum dot enhanced GaAs solar cells, Appl. Phys. Lett. 92 (2008) 123512.
[16] R. Oshima, A. Takata, Y. Okada, Strain-compensated InAs/GaNAs quantum dots for use in high-efficiency solar cells, Appl. Phys. Lett. 93 (2008) 83111.
[17] D. Guimard, R. Morihara, D. Bordel, K. Tanabe, Y. Wakayama, M. Nishioka, Y. Arakawa, Fabrication of InAs/GaAs quantum dot solar cells with enhanced photocurrent and without degradation of open circuit voltage, Appl. Phys. Lett. 96 (2010) 203507.
[18] S.M. Hubbard, C.G. Bailey, R. Aguinaldo, S. Polly, D.V. Forbes, R.P. Raffaelle, Characterization of quantum dot enhanced solar cells for concentrator photovoltaics, in: Proceedings of the 34th IEEE Photovoltaics Specialists Conference, 2009.
[19] P.G. Linares, A. Martí, E. Antolí, C.D. Farmer, I. Ramiro, C.R. Stanley, A. Luque, Voltage recovery in intermediate band solar cells, Sol. Energy Mater. Sol. Cells 98 (2012) 240–244.
[20] R.A. Sinton, A. Cuevas, A quasi-steady-state open-circuit voltage method for solar cell characterisation, in: Proceedings of the 16th European Photovoltaic Solar Energy Conference, 2000.
[21] S.M. Willis, J.A.R. Dimmock, F. Tutu, H.Y. Liu, M.G. Peinado, H.E. Assender, A.A. R. Watt, I.R. Sellers, Defect mediated extraction in InAs/GaAs quantum dot solar cells, Sol. Energy Mater. Sol. Cells 102 (2012) 142–147.
[22] Z. Wasilewski, S. Farfad, J. McCaffrey, Size and shape engineering of vertically stacked self-assembled quantum dots, J. Cryst. Growth 201–202 (2006) 1131–1135.
[23] T. Sogabe, Y. Shoji, M. Ohba, K. Yoshida, R. Tamaki, H.-F. Hong, C.-H. Wu, C.-T. Kuo, S. Tomić, Y. Okada, Intermediate-band dynamics of quantum dots solar cell in concentrator photovoltaic modules, Sci. Rep. 4 (2014) 4792.
[24] T. Li, R.E. Bartolo, M. Dagenais, Challenges to the concept of an intermediate band in InAs/GaAs quantum dot solar cells, Appl. Phys. Lett. 103 (2013) 141113.
[25] G. Jolley, H.F. Lu, L. Fu, H.H. Tan, C. Jagadish, Electron–hole recombination properties of $In_{0.5}Ga_{0.5}As$/GaAs quantum dot solar cells and the influence on the open circuit voltage, Appl. Phys. Lett. 97 (2010) 123505.
[26] A. Martí, A. Luque, Next Generation Photovoltaics: High Efficiency Through Full Spectrum Utilization, IOP Publishing, Bristol, UK, 2004.
[27] H.F. MacMillan, H.C. Hamaker, N.R. Kaminar, J.M. Gee, M.S. Kuryla, M. Ladle, D.D. Liu, G.F. Virshup, 28% efficient GaAs concentrator solar cells, in: Proceedings of the 20th IEEE Photovoltaics Specialists Conference, 1988.
[28] O. Breitenstein, S. Rißland, A two-diode model regarding the distributed series resistance, Sol. Energy Mater. Sol. Cells 110 (2013) 77–86.
[29] T. Gu, M.A. El-Emawy, K. Yang, A. Stintz, L.F. Lester, Resistance to edge recombination in GaAs-based dots-in-a-well solar cells, Appl. Phys. Lett. 95 (2009) 261106.